J. Micromech. Microeng. **17** (2007) S211–S216 doi:10.1088/0960-1317/17/9/S01

# Performance limits of the three MEMS inertial energy generator transduction types

**P D Mitcheson[1], E K Reilly[2], T Toh[1], P K Wright[2] and E M Yeatman[1]**

[1] Department of Electrical and Electronic Engineering, Imperial College, London, UK
[2] Department of Mechanical Engineering, University of California, Berkeley, CA, USA

E-mail: paul.mitcheson@imperial.ac.uk

Received 14 February 2007, in final form 10 April 2007
Published 31 August 2007
Online at stacks.iop.org/JMM/17/S211

**Abstract**
In this paper, trends from the last 10 years of inertial micro-generator literature are investigated and it is shown that, although current generator designs are still operating well below their maximum power, there has been a significant improvement with time. Whilst no clear conclusions could be drawn from reported fabricated devices with respect to preferred transducer technology, this paper presents operating charts for inertial micro-generators which identify optimal operating modes for different frequencies and normalized generator sizes, and allows comparison of the different transduction mechanisms as these parameters vary. It is shown that piezoelectric generators have a wider operating range at low frequency than electromagnetic generators, but as generator dimensions increase, the frequency to which piezoelectric transducers outperform electromagnetic transducers decreases.

(Some figures in this article are in colour only in the electronic version)

## 1. Introduction

Motion and vibration are attractive sources for micro-engineered energy scavenging generators [1, 2]. The most universal motion scavengers are of the inertial type, i.e. having a proof mass suspended within a frame and energy extracted by a transducer that damps the motion of the proof mass within the frame. These devices have the advantage that they can function simply by being attached to a source of motion at a single point, rather than relying on the relative motion of different parts of the 'host' structure. Thus they are also well suited to miniaturization.

The basic operating principle of inertial micro-generators is illustrated in figure 1. The fundamental parameters limiting the generator output are its proof mass $m$ and maximum internal displacement $Z_l$, and the source motion amplitude $Y_0$ and frequency $\omega$ [3]. From these we can derive the maximum power from basic principles. If we assume harmonic source motion, the maximum acceleration $a_{max}$ is $\omega^2 Y_0$. The maximum damping force by which energy can be extracted is equal to the inertial force on the proof mass, $ma_{max}$ (if greater, the mass will not move relative to the frame). If energy is extracted in both directions, and the internal motion amplitude $Z_0 = Z_l$ (giving the maximum travel range of $2Z_l$), we derive a total energy per cycle of $4Z_l ma_{max} = 4Z_l m\,\omega^2 Y_0$. To convert this to power we simply divide by the excitation period $2\pi/\omega$, giving

$$P_{max} = 2Y_0 Z_l \omega^3 m/\pi. \quad (1)$$

We can then define a normalized power $P_n = P/P_{max}$ as a measure of how close the performance of a specific device comes to the optimum level. We have calculated $P_n$ for *measurements* on inertial energy scavengers reported in the literature [1, 4–27] and the resulting values are plotted in figure 2 as a function of the year of publication. An upward trend can clearly be seen, although the best values are still below 20% of the optimum. Although $P_n$ should not drop with volume, since it is normalized to device size, the same data plotted against device volume (figure 3) show that typically the best $P_n$ values have been achieved for larger devices.

  

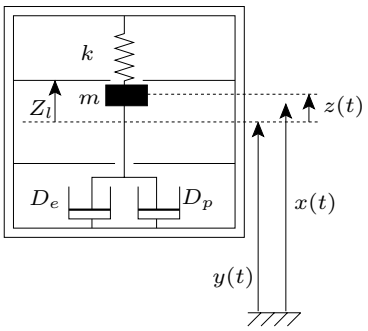


**Figure 1.** Schematic construction of inertial generators.

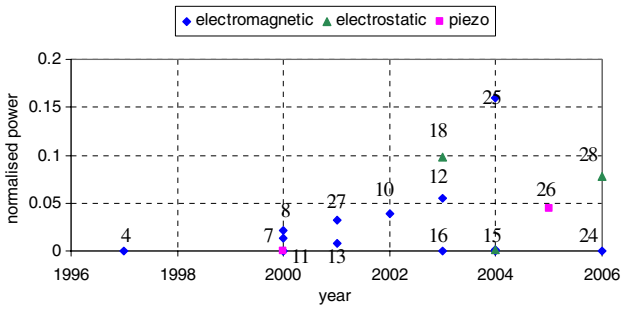


**Figure 2.** Normalized measured power $P_n$ versus year of publication. Numbers show which reference the data were taken from.

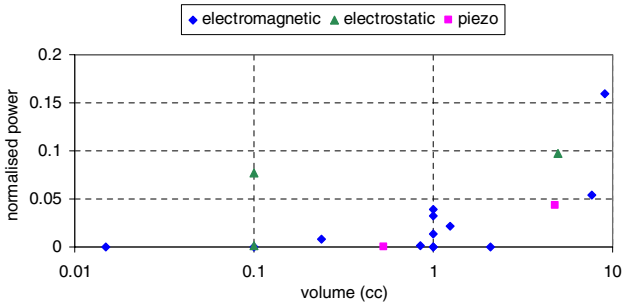


**Figure 3.** Normalized measured power $P_n$ versus device volume.

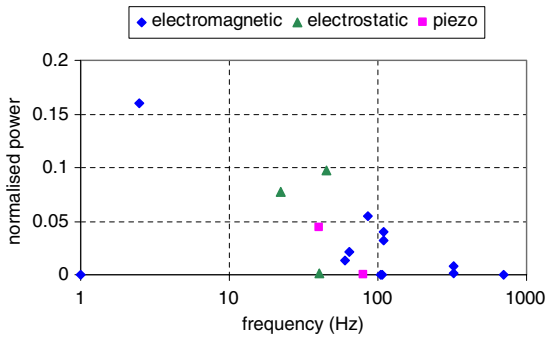


**Figure 4.** Normalized measured power $P_n$ versus operating frequency.

This is likely an indication of the technological difficulties encountered at smaller size scales, for example the greater difficulty in achieving high magnetic flux gradients. Finally, we plot the normalized power versus frequency (figure 4), and a downward trend is clearly seen.

Several transduction mechanisms can be used for inertial micro-generators, namely electromagnetic [14], electrostatic [28] and piezoelectric [29]. The transduction type is also indicated in figures 2–4, but no clear trends can be seen regarding their relative merits. To obtain some general guidance on the practical limitations of specific transduction methods, we have examined the key issue of the damping levels that can be achieved. We consider only mechanically resonant devices operating at the resonant frequency $\omega_n$, as this covers most reported examples.

## 2. Scaling analysis of transducer types

In an ideal case, the parasitic damping would be zero, and maximum power is then obtained by setting the electrical damping factor $\zeta_e$ to the level that allows the mass to move over the entire internal range, but without hitting the end stops, i.e. $Z_0 = Z_l$ [3]. However, in some cases the maximum damping force of the transducer is insufficient to achieve this, and thus the device cannot operate in a resonant mode. In cases where the parasitic damping factor $\zeta_p$ is not negligible, maximum power will inevitably be reduced, but the optimum $\zeta_e$ will still be that which gives $Z_0 = Z_l$, unless this requires $\zeta_e < \zeta_p$, in which case $\zeta_e = \zeta_p$ should be chosen if possible.

In general, the damping factor is related to the resonant quality factor $Q$ by $Q = 1/2\zeta$. Since the damping will have parasitic and electrical (transducer) components, we introduce the quantities $Q_p = 1/2\zeta_p$ and $Q_e = 1/2\zeta_e$. Note that the combined $Q$ is given by $1/Q = 1/Q_p + 1/Q_e$. Furthermore, for a resonant system in which the damping force is proportional to the relative mass-frame velocity, i.e. $F = -D\mathrm{d}z/\mathrm{d}t$, $D = 2m\omega_n\zeta$. To perfectly damp the system we require $Q = Z_l/Y_0$, so that $D = m\omega_n/(Z_l/Y_0)$.

### 2.1. Electromagnetic damping

An electromagnetic damper can be implemented as a coil moving across the boundary of a region of magnetic flux density $B$. If we assume that the induced voltage is limited mainly by the resistive load $R$, rather than the coil's inductance, then in this case the electrical damping coefficient is given by $D_e = (NBl)^2/R$ [3], where $N$ is the number of coil turns and $l$ is the length of the border of the flux region cutting across the coil. The load $R$ will consist of the coil resistance $R_i$ (which is a parasitic component) and the energy extracting load $R_L$ in series. The former determines the maximum $D_e$, and thus the minimum $Q_e$; however, unless $R_L$ is substantially greater than $R_i$ most of the electrical power will be wasted. Instead we assume that a useful device has at least $R_L = 10R_i$. This sets the minimum achievable $Q_e$ as

$$Q_e(\min) \approx \frac{10mR_i}{(NBl)^2}\omega_n. \qquad (2)$$

If this quantity is greater than $Z_l/Y_0$, it will not be possible to achieve harmonic motion by electrical damping alone, although it may be possible if significant parasitic mechanical damping is present. A key implication of (2) is that the range of achievable $Q_e$ reduces with increasing frequency.

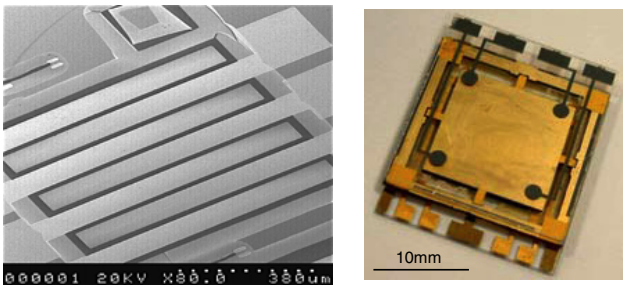


**Figure 5.** Prototype MEMS inertial scavengers: piezoelectric (left) and electrostatic (right).

### 2.2. Piezoelectric damping

A similar quantity can be derived for the piezoelectric case. We start with the constituent equations for the piezoelectric cell [30]:

$$F_{\mathrm{p}} = K_{\mathrm{PE}} z + \alpha V \tag{3}$$

$$I = \alpha \dot{z} - C_0 \dot{V}. \tag{4}$$

Here $F_{\mathrm{p}}$ is the force produced by the piezoelectric material, $V$ is the voltage between the terminals, $I$ is the current through the terminals, $K_{\mathrm{PE}}$ is the short circuit stiffness, $z$ is the relative displacement, $C_0$ is the capacitance of the piezoelectric element and $\alpha = e_{33} A/t$, with $A$ and $t$ being the cross-sectional area and thickness of the piezo element respectively, and $e_{33}$ is the piezoelectric coefficient. Note that $e_{33}$ applies to the case where the voltage and strain are colinear; many implementations, such as thin piezo films on cantilevers, have strain and electric field on orthogonal axes, and an off-diagonal element of the piezoelectric tensor then applies in place of $e_{33}$. The force developed by the piezoelectric cell with a resistive load $R$ connected can be found from these equations, in the Laplace domain, as

$$F(s) = Z(s)\left(K_{\mathrm{PE}} + \frac{s\alpha^2 R}{1 + sC_0 R}\right). \tag{5}$$

The force developed by the piezoelectric material is therefore a constant spring force plus a force which acts as a first-order high pass filter. The frequency response, $F_{\mathrm{HP}}(j\omega)$, of the high pass filter term is

$$F_{\mathrm{HP}}(\mathrm{j}\omega) = Z(\mathrm{j}\omega)\left(\frac{\mathrm{j}\omega\alpha^2 R}{1 + \mathrm{j}\omega C_0 R}\right) \tag{6}$$

which can be written as

$$F_{\mathrm{HP}}(\mathrm{j}\omega) = Z(\mathrm{j}\omega)\left(\frac{\mathrm{j}\omega\alpha^2 R}{1 + (\omega C_0 R)^2} + \frac{\omega^2\alpha^2 C_0 R^2}{1 + (\omega C_0 R)^2}\right). \tag{7}$$

These terms are therefore a frequency-dependent damping term (proportional to $\mathrm{j}\omega Z(\mathrm{j}\omega)$) and a frequency-dependent spring constant term (proportional to $Z(\mathrm{j}\omega)$). The resistance can be altered to maximize the available damping force, $F_{\mathrm{D}}(\mathrm{j}\omega)$, i.e. when

$$\frac{\mathrm{d}F_{\mathrm{D}}(\mathrm{j}\omega)}{\mathrm{d}R} = 0, \tag{8}$$

which is when

$$R = \frac{1}{\omega C_0}. \tag{9}$$

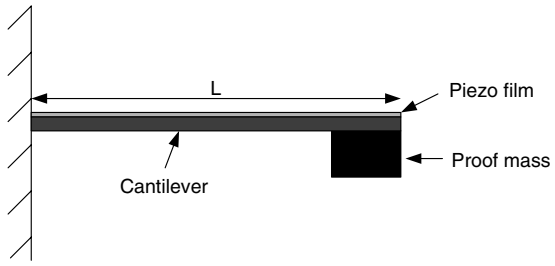


**Figure 6.** Piezoelectric film on a cantilever beam.

Thus,

$$D_{\max} = \frac{\alpha^2}{2\omega C_0}. \tag{10}$$

In practice, since piezo-elements can only achieve very small direct displacements, devices must incorporate some leverage mechanism (of ratio $r$). A typical example is the cantilever structure shown in figure 6. If we approximate this as a thin film of piezoelectric material on a structural cantilever of thickness $h$, then it is straightforward to show that the proof mass motion $\Delta z$ is greater than the piezo-film extension (or compression) by a factor $L/h$.

The leverage will transform the damping coefficient (i.e. the force to velocity ratio) by a factor of $r^2$, in a manner equivalent to an electrical transformer of turn ratio $r$. Thus we obtain

$$Q_{\mathrm{e}}\,(\min) = \frac{2mC_0 r^2}{\alpha^2}\omega_{\mathrm{n}}^2. \tag{11}$$

Since the other parameters in this expression have little or no frequency dependence, the minimum $Q_{\mathrm{e}}$ is proportional to the frequency squared. Thus the operating range for which optimum power can be achieved becomes rapidly diminished with increasing frequency, more rapidly than in the electromagnetic case considered above.

### 2.3. Electrostatic damping

For the case of the electrostatic damper, the damping is nonlinear but a closed-form solution to the minimum available $Q$ factor exists. This is given in [3] as

$$Q_{\mathrm{e}}(\min) = \omega_{\mathrm{c}}^2\left[\frac{1}{\left(1-\omega_{\mathrm{c}}^2\right)^2} - \left(\frac{F_{\max}}{mY_0\omega^2\omega_{\mathrm{c}}}U\right)^2\right]^{\frac{1}{2}} \tag{12}$$

where

$$U = \frac{\sin\left(\frac{\pi}{\omega_{\mathrm{c}}}\right)}{1 + \cos\left(\frac{\pi}{\omega_{\mathrm{c}}}\right)}. \tag{13}$$

There are two different methods of operating an electrostatic transducer to achieve Coulomb (fixed force) damping, which are gap-closing constant charge operation and sliding plate constant voltage operation. The most common type on the microscale is the latter, in the form of a comb drive variable capacitor on a folded suspension. For this type of transducer the parasitic damping force can be approximated as [31]

$$F_{\mathrm{p}}(\dot{z}) = \frac{2N_{\mathrm{g}} t \mu_{\mathrm{air}} x_0}{g}\dot{z}. \tag{14}$$

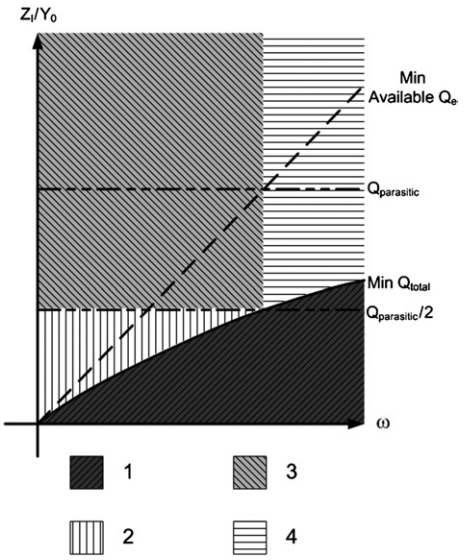


**Figure 7.** Operating limits on the electrical damping and parasitic $Q$ factor.

Here $N_g$ is the number of gaps in the comb drive, $t$ is the thickness of the structure, $\mu_{air}$ is the viscosity of air, $g$ is the gap width, $x_0$ is the initial gap overlap and $z$ is the overlap movement. The electrical damping force is given by

$$F_e(z) = \frac{Q_c^2}{2C_0}\frac{1}{(z+x_0)^2} \tag{15}$$

where $Q_c$ is the initial charge on the capacitor and $C_0$ is the capacitance per given length as given by

$$C_0 = \frac{N_g \varepsilon_0 t}{g}. \tag{16}$$

It can be seen that the electrical damping force is not proportional to velocity, as is required for a harmonic oscillation. Thus the motion will be inherently nonlinear. Furthermore, it is a property of Coulomb damped resonators that when operated at the resonant frequency, in the absence of parasitic damping and physical stops, the motion amplitude rises without limit unless the damping force satisfies a stability criterion [32]:

$$F_e \geqslant \frac{\pi}{4} m\omega^2 Y_0. \tag{17}$$

### *2.4. Example operating chart*

If we define $Z_l/Y_0$ and $\omega_n$ as our general operating parameters, then we can plot equations (2) and (11) as limits of operation for electromagnetic and piezoelectric devices. By adding the $Q_p$ of the device, and the combined $Q$, we can indicate regions of operation as a function of the operating point.

This is done in figure 7 schematically, for an electromagnetic generator with parasitic damping present. The parasitic damping factor (and hence the $Q_p$) has been assumed to be constant with frequency for simplicity, but any actual frequency dependence could easily be substituted. For example, the parasitic damping force for a comb drive as given by equation (14) is equivalent to a frequency-independent damping coefficent $D$, and thus a $Q_p$ linearly proportional to frequency.

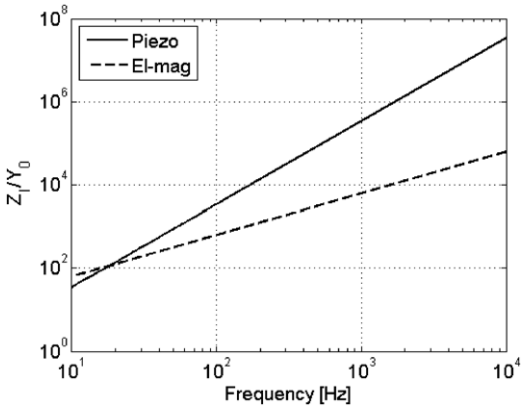


**Figure 8.** Comparison of minimum $Q$ factors with electromagnetic and piezoelectric cube devices of volume 1 cc.

With reference to figure 7, the operating regions are as follows:

1. Harmonic motion is not possible. The maximum combined damping factor (which is $(1/Q_p + 1/Q_e)$) is less than required for oscillation within the limit of $Z_l$. The line marked 'minimum $Q_{total}$' indicates the minimum value of $Z_0/Y_0$ achievable. If the operating point is below this line, harmonic motion is not possible and the mass will strike the end stops.
2. Optimal operation occurs when the electrical damping and parasitic damping are equal, assuming that this results in $Z_0 < Z_l$. In this operating region, if the parasitic and electrical damping terms were set equal, i.e. $Q_e = Q_p$, the mass would hit the end stops because the overall damping would not be large enough. Therefore, for optimal operation, the electrical damping should be set so that $Z_0 = Z_l$, i.e. $Q_e > Q_p$.
3. In this region of the figure, the parasitic and electrical damping terms should be set equal, i.e. $Q_e = Q_p$. The device will then operate within its displacement limit. This will give $Z_0/Y_0 = Q_{parasitic}/2$.
4. In this region it is not possible to make the electrical damping and parasitic damping equal, because the electrical damping force cannot be made large enough, i.e. $Q_e > Q_p$. The electrical damping should therefore be set to the maximum that can be achieved. The generator can operate within the displacement constraint, but a different transducer could in principle extract more power if it could generate a higher damping force.

Figures 8 and 9 show two specific examples of the minimum $Q$-factor achievable from electromagnetic and piezoelectric generators. In each case we assume a cubic device of length $L$ and the mass , of relative density 8.9 (Ni), is taken to occupy half the device volume. The electromagnetic device is assumed to have a flux density of 1 T and a copper coil occupying 2% of the device volume, for which a fixed $N^2/R_i$ is obtained. The active coil length $l$ is assumed to be $L/2$. For the piezoelectric device, we assume $\varepsilon_r = 1000$, area $L^2$, thickness $L/10$ and $e_{33} = 0.15$ C m$^{-2}$. A leverage factor of 500 was chosen. Because $Q_{min}$ for electromagnetic and piezoelectric devices scale as $\omega$ and $\omega^2$ respectively, there will always be a frequency above which electromagnetic devices can achieve

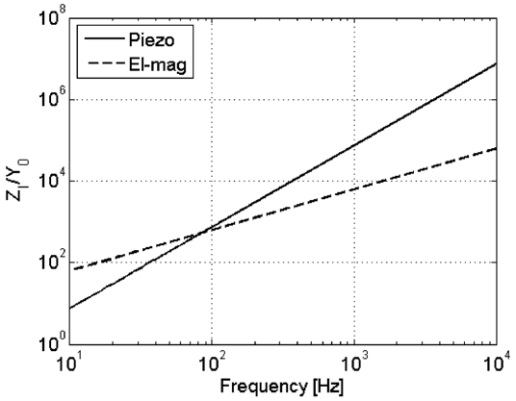


**Figure 9.** Comparison of minimum $Q$ factors with electromagnetic and piezoelectric cube devices of volume 0.1 cc.

higher damping. As can be seen in figures 8 and 9, the cross-over frequency increases as the device size decreases. It can also be observed that the increasing $Q$ with frequency (for both transducer types) could explain the decreasing performance trend seen in figure 4.

## 3. Conclusions

Obtaining maximum power from inertial energy scavengers is often limited by the maximum damping force achievable in the transduction mechanism, and this problem increases with increasing frequency. Piezoelectric generators can outperform electromagnetic generators at low frequency, but with increasing frequency, the internal capacitance of the piezoelectric reduces the amount of real power that can be obtained. This suggests that piezoelectric devices might be better suited to human body powered applications and electromagnetic devices to high frequency applications.

## References


[1] Roundy S, Wright P K and Rabaey J M 2003 *Energy Scavenging for Wireless Sensor Networks* (Boston, MA: Kluwer)

[2] Paradiso J A and Starner T 2005 Energy scavenging for mobile and wireless electronics *IEEE Pervasive Comput.* **4** 18–27

[3] Mitcheson P D, Green T C, Yeatman E M and Holmes A S 2004 Architectures for vibration-driven micropower generators *J. Microelectromech. Syst.* **13** 429–40

[4] Shearwood C and Yates R B 1997 Development of an electromagnetic microgenerator *Electron. Lett.* **33** 1883–4

[5] Williams C B, Shearwood C, Harradine M A, Mellor P H, Birch T S and Yates R B 2001 Development of an electromagnetic micro-generator *IEEE Proc.* G **148** 337–42

[6] Li W J, Chan G M H, Ching N N H, Leong P H W and Wong H Y 2000 Dynamical modelling and simulation of a laser-micromachined vibration-based micro power generator *Int. J. Nonlinear Sci. Simul.* **1** 345–53

[7] Li W J, Ho T C H, Chan G M H, Leong P H W and Wong H Y 2000 Infrared signal transmission by a laser-micromachined, vibration-induced power generator *Proc. 43rd IEEE Midwest Symp. on Circuits and Systems (2000)*

[8] Li W J, Wen Z, Wong P K, Chan G M H and Leong P H W 2000 A micromachined vibration-induced power generator for low power sensors or robotic systems *8th Int. Symp.on Robotics with Applications (HI)*

[9] Ching N N H, Chan G M H, Li W J, Wong H Y and Wen Z 2000 A laser-micromachined vibrational to electrical power transducer for wireless sensing systems *11th Int. Conf. Solid-State Sensors and Actuators (Munich, Germany)*

[10] Ching N 2002 A laser-micromachined multi-modal resonating power transducer for wireless sensing systems *Sensors Actuators* A **97** 685

[11] Ching N N H, Chan G M H, Li W J, Wong H Y and Leong P H W 2000 PCB integrated micro-generator for wireless systems *Int. Symp. Smart Structures (Hong Kong)*

[12] Lee J M H, Yuen S C, Li W J and Leong P H W 2003 Development of an AA size energy transducer with micro-resonators *Int. Symp. Circuits and Systems*

[13] El-hami M, Glynne-Jones P, White N M, Hill M, Beeby S, James E, Brown A D and Ross J N 2001 Design and fabrication of a new vibration-based electromechanical power generator *Sensors Actuators* A **92** 335–42

[14] Glynne-Jones P, Tudor M J, Beeby S P and White N M 2004 An electromagnetic, vibration-powered generator for intelligent sensor systems *Sensors Actuators* A **110** 344–9

[15] Kulah H and Najafi K 2004 An electromagnetic micro power generator for low-frequency environmental vibrations, *17th IEEE Int. Conf. on Micro Electro Mechanical Systems (MEMS) (2004)*

[16] Mizuno M and Chetwynd D G 2003 Investigation of a resonance microgenerator *J. Micromech. Microeng.* **13** 209–16

[17] Miyazaki M, Tanaka H, Ono G, Nagano T, Ohkubo N and Kawahara T 2004 Electric-energy generation using variable-capacitive resonator for power-free-LSI *IEICE Trans. Electron.* **E87-C** 549–55

[18] Miyazaki M, Tanaka H, Ono G, Nagano T, Ohkubo N, Kawahara T and Yano K 2003 Electric-energy generation using variable-capacitance resonator for power-free LSI: efficiency analysis and fundamental experiment *Int. Symp. on Low Power Electronics and Design*

[19] Mitcheson P D, Miao P, Stark B H, Yeatman E M, Holmes A S and Green T C 2004 MEMS electrostatic micropower generator for low frequency operation *Sensors Actuators* A **115** 523–9

[20] Glynne-Jones P, El-hami M, Beeby S, James E, Brown A D, Hill M and White N M 2000 A vibration-powered generator for wireless microsystems *Int. Symp. on Smart Structures and Microsystems*

[21] Glynne-Jones P, Beeby S P and White N M 2001 Towards a piezoelectric vibration-powered microgenerator *IEE Proc. Sci. Meas. Technol.* **148** 68–72

[22] White N M, Glynne-Jones P and Beeby S P 2001 A novel thick-film piezoelectric micro-generator *Smart Mater. Struct.* **10** 850–2

[23] Glynne-Jones P, Beeby S, James E and White N M 2001 The modelling of a piezoelectric vibration powered generator for microsystems *Transducers '01, Eurosensors XV (Munich, Germany)*

[24] Koukharenko E, Beeby S P, Tudor M J, White N M, O'Donnell T, Saha C, Kulkarni S and Roy S 2006 Microelectromechanical systems vibration powered electromagnetic generator for wireless sensor applications *Microsyst. Technol. Micro Nanosyst. Inform. Storage Process. Syst.* **12** 1071–7

[25] Duffy M and Carroll D 2004 Electromagnetic generators for power harvesting *IEEE 35th Ann. Power Electronics Specialists Conf. (2004): PESC 04*

[26] Hammond K, Leland E S, Baker J, Carleton E, Reilly E, Lai E, Otis B, Rabaey J M, Sundararajan V and Wright P K 2005 An integrated node for energy-scavenging, sensing and data transmission: applications in medical diagnostics *2nd Int. Workshop on Wearable and Implantable Body Sensor Networks (Imperial College, London)*

[27] Ching N 2001 A laser-micromachined multi-modal resonating power transducer for wireless sensing systems *11th Int.*

*Conf. on Solid State Sensors and Actuators (Munich, Germany)*

[28] Miao P, Mitcheson P D, Holmes A S, Yeatman E M, Green T C and Stark B H 2006 MEMS inertial power generators for biomedical applications *Microsyst. Technol. Micro Nanosyst. Inform. Storage Process. Syst.* **12** 1079–83

[29] Reilly E K, Carleton E and Wright P K 2006 Thin film piezoelectric energy scavenging systems for long term medical monitoring *Int. Workshop on Wearable and Implantable Body Sensor Networks (2006): BSN 2006*

[30] Guyomar D, Badel A, Lefeuvre E and Richard C 2005 Toward energy harvesting using active materials and conversion improvement by nonlinear processing *IEEE Trans. Ultrason. Ferroelectr. Freq. Control* **52** 584–95

[31] Borovic B, Lewis F L, Liu A Q, Kolesar E S and Popa D 2006 The lateral instability problem in electrostatic comb drive actuators: modeling and feedback control *J. Micromech. Microeng.* **16** 1233

[32] Den Hartog J P 1985 *Mechanical Vibrations* (Mineola, NY: Dover)